Table XI. Enthalpies of Transfer of Solutes from *n*-Hexane and 1-Octanol to Water (in kcal mol^{-1}) at 298 K[a]

solute	1-octanol → water	*n*-hexane → water
O_2	−2.60	−2.65
CH_4	−2.37	−2.76
C_2H_6		−2.73
C_3H_8		−2.01
n-C_4H_{10}		−1.31
n-C_5H_{12}		−0.11
n-C_6H_{14}		0.04
n-C_7H_{16}		0.64
Me_4Sn	−0.86	−0.70

[a] Values from Tables IV and VI.

favorable) entropic term is rather small.

Finally, I refer to the suggestion of Wertz[16] that it is possible to calculate partition coefficients or $\Delta G°_t$ values for transfer of solutes from nonaqueous solvents to water on the assumption that the corresponding $\Delta H°_t$ values are zero. Wertz[16] applied this assumption in the calculation of values of $\Delta G°_t$ for transfer of methane, ethane, propane, and *n*-butane from 1-octanol to water. In Table XI are listed the $\Delta H°_t$ values for transfer of solutes from 1-octanol and *n*-hexane to water. It is clear that the $\Delta H°_t$ values can be so far from zero that Wertz' assumption cannot be at all generally valid. In any case, it is now possible to obtain the required $\Delta G°_t$ values either from the observed $\Delta G°_s$ values in Tables I and IV or from $\Delta G°_s$ values estimated through the correlations in Table III. The other suggestion of Wertz,[16] that all molecules lose the same fraction of their entropy on solution in water, has already been shown not to be generally valid.[57]

Registry No. He, 7440-59-7; Ne, 7440-01-9; Ar, 7440-37-1; Kr, 7439-90-9; Xe, 7440-63-3; Rn, 10043-92-2; H_2, 1333-74-0; N_2, 7727-37-9; CO, 630-08-0; O_2, 7782-44-7; CH_4, 74-82-8; C_2H_6, 74-84-0; C_3H_8, 74-98-6; n-C_4H_{10}, 106-97-8; n-C_5H_{12}, 109-66-0; n-C_6H_{14}, 110-54-3; n-C_7H_{16}, 142-82-5; n-C_8H_{18}, 111-65-9; CF_4, 75-73-0; SF_6, 2551-62-4; Me_4C, 463-82-1; Me_4Sn, 594-27-4; Et_4C, 1067-20-5; Et_4Sn, 597-64-8; Et_4Pb, 78-00-2; isobutane, 75-28-5; cyclopentane, 287-92-3; cyclohexane, 110-82-7.

(57) M. H. Abraham, *J. Am. Chem. Soc.*, **103**, 6742 (1981).

Photochromic Forms of 6-Nitrobenzospiropyran. Emission Spectroscopic and ODMR Investigations

M. Gehrtz, Chr. Bräuchle,* and J. Voitländer

Contribution from the Institut für Physikalische Chemie der Universität München, D-8000 München 2, West Germany. *Received July 1, 1981*

Abstract: The photochromic compound 6-nitrobenzopiropyran was investigated by luminescence and ODMR spectroscopic techniques at temperatures $T \leq 4.2$ K. The data are discussed with respect to a model based on a calculation of charge-transfer wave functions. Both the uncolored A form and the long suspect X form could be identified, and the properties of their triplet state were determined, i.e. phosphorescence, zero-field splitting, and the selective kinetics of population and deactivation (radiative and radiationless) of the triplet zero-field levels. By symmetry arguments, these data indicate that the triplet states of the A and the X form are of $\pi\pi^*$ nature and surprisingly belong to the point group C_{2v}. This is in excellent agreement with the calculation which showed that the nitrochromene part of the molecule can be considered as a para-disubstituted benzene subunit, the wave function of which exhibits considerable charge-transfer character. On the basis of this theory, the vibrational analysis of the phosphorescence with its strong solvent dependence as well as the zero-field splitting can be explained qualitatively and quantitatively. The results can serve as a guideline for future investigations of the detailed photochemical reactivity of 6-nitrobenzospiropyran.

Since its discovery in 1953,[1] the photochromism of spiropyrans has been extensively investigated with mainly four aims: (i) use for optical storage of data or for phototropic glasses,[2] (ii) elucidation of the excited states involved in the photochromic process and their chemical and physical properties,[2,3] (iii) modeling the role of natural chromenes in the photoregulation of biological processes in plants,[4] (iv) and use as a probe for specific investigations of bulk polymers.[5]

This paper deals with topic ii of the above enumeration, especially with the physical properties of the lowest excited triplet state T_1 of 6-nitrobenzospiropyran (6-NB). These are prerequisite data[6] to subsequent work of this laboratory on the detailed chemical kinetics of triplet photoreactions,[7] the aim of which is to show that the triplet sublevels (zero-field levels) possess individual chemical reactivities—just as is the case for the various photophysical processes involving T_1.[8,9]

Here we present the results of the investigation of the photophysical parameters of 6-NB carried out with the help of emission spectroscopic and ODMR techniques. It is shown that the various photochromic forms—under the very low temperature conditions used throughout—can be identified from the spectra, even the long-suspect intermediate form X.[10] The symmetry properties and the electronic nature of both the uncolored and the inter-

(1) Chaude, O.; Rumpf, P. *C. R. Hebd. Seances Acad. Sci.* **1953**, *236*, 697-699.
(2) Bertelson, R. C. *Tech. Chem. (N.Y.)* **1971**, *3*, 49-288.
(3) Arnaud, J.; Wippler, C.; Beaure d'Augeres, F. *J. Chim. Phys.* **1967**, *64*, 1165-1173. Metras, J.-C.; Mossé, M.; Wippler, C. *Ibid.* **1965**, *62*, 559-672.
(4) Bārta, M. *Coll. Czech. Chem. Commun.* **1978**, *43*, 3339-3346.
(5) Eisenbach, C. D. *Ber. Bunsenges. Phys. Chem.* **1980**, *84*, 680-690.
(6) Gehrtz, M.; Bräuchle, Chr.; Voitländer, J. *Z. Naturforsch. A* **1981**, *36*, 743-750.
(7) Gehrtz, M.; Bräuchle, Chr.; Voitländer, J., in preparation.
(8) Lawetz, V.; Orlandi, G.; Siebrand, W. *J. Chem. Phys.* **1972**, *56*, 4058-4072. Metz, F.; Friedrich, S.; Hohlneicher, G. *Chem. Phys. Lett.* **1972**, *16*, 353-358.
(9) El-Sayed, M. A. *Annu. Rev. Phys. Chem.* **1975**, *26*, 235-258. *Acc. Chem. Res.* **1971**, *4*, 23-31.
(10) Heiligman-Rim, R.; Hirshberg, Y.; Fischer, E. *J. Phys. Chem.* **1962**, *66*, 2470-2477.

0002-7863/82/1504-2094$01.25/0

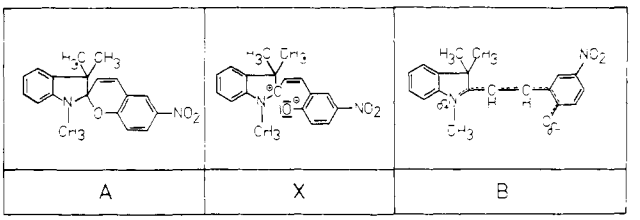

Figure 1. Photochromic forms of 6-NB: (A) uncolored spiro form; (X) intermediate form; (B) colored merocyanine form.

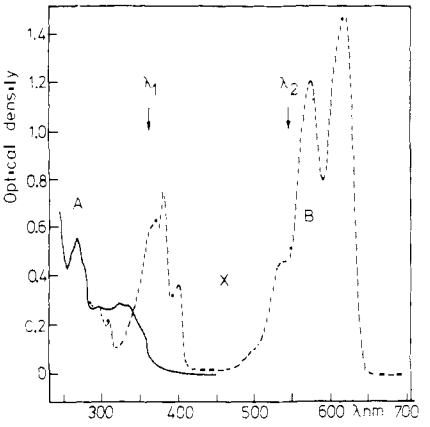

Figure 2. Absorption spectra of the photochromic forms of 6-NB in nonpolar solvents. Spectra of A and B taken from ref 12, spectrum of X taken from ref 13. For the meaning of λ_1 and λ_2, cf. eq 1. The influence of irradiation at λ_1 on the backreaction X → A is not yet clear.

mediate form, as revealed by the ODMR method, are discussed with respect to a consistent model based on a calculation of charge-transfer wave functions.

1. Photochromic Forms

The structural formulas of 6-NB are presented in Figure 1. In the uncolored form A, the indoline and chromene parts of the molecule are orthogonal, and the absorption spectrum is governed by local excitations within the two parts,[11] whereas in the colored B form, the molecule is planar and displays the long wavelength absorption typical for merocyanine dyes[12] (cf. Figure 2). When irradiating at wavelength λ_1, the primary photochemical step in ring opening (A → B) is the rupture of the bond between the spiro C atom and the pyran oxygen—i.e., the formation of the X form where the orthogonal topology still is retained.[10] Note that then the sp^3 hybridization of C_{spiro} is conserved. Therefore, the positive charge has to be located at C_{spiro} and not at the nitrogen of the indoline part—as is the case for the B form. Consecutive thermal steps leading to the various isomers of the B form[3,10,12] as well as thermal interconversions among them are frozen out at temperatures below 90 K[12] and therefore are of no concern for the low-temperature (4.2 K) in this study.

The existence of the intermediate X was postulated by an Israeli group[12] but could not be proved from their conventional spectroscopic data. With the help of nanosecond laser spectroscopy, Russian researchers found a short-lived absorption centered around 440 nm (cf. Figure 2).[13] Even though not quite unambiguous, we will use their assignment of this band to the X form for further discussions. It will be in excellent agreement with all results of this work.

In summary, the forward and backward reaction can be described by the following scheme (cf. Figure 2):

$$A \underset{\lambda_1(?)}{\overset{\lambda_1}{\rightleftharpoons}} X \underset{\lambda_2,\ \lambda_1}{\overset{kT,\ \lambda_1}{\rightleftharpoons}} B \qquad (1)$$

(11) Tyer, N. W., Jr.; Becker, R. S. *J. Am. Chem. Soc.* **1970**, *92*, 1289–1294, 1295–1302.
(12) Bercovici, R.; Heiligman-Rim, R.; Fischer, E. *Mol. Photochem.* **1969**, *1*, 23–55.
(13) Murin, V. A.; Mandzhikov, V. A.; Barachevskii, V. A. *Opt. Spectrosc. (USSR)* **1974**, *37*, 685–676.

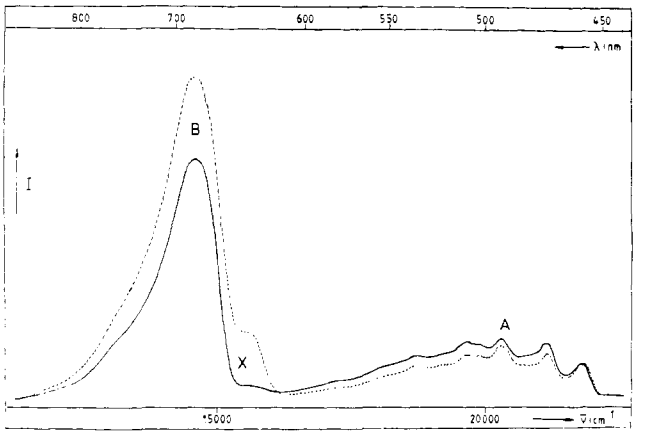

Figure 3. Emission spectrum of 6-NB in 3-MP. The spectral regions are attributed to the photochromic forms A, X, and B. Broken line: spectrum after ca. 2-h irradiation at T = 4.2 K, λ_{exc} = 365 nm.

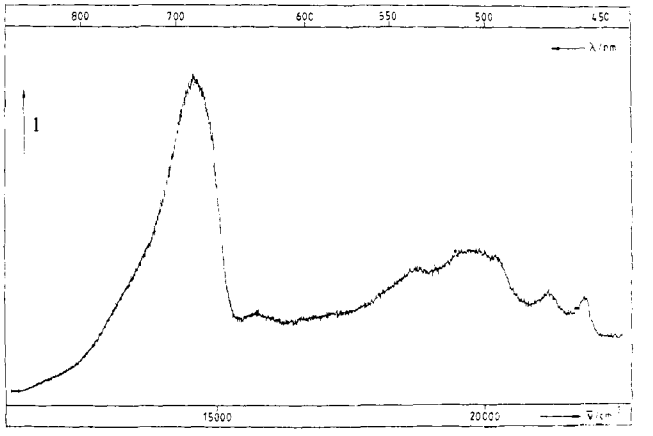

Figure 4. Emission spectrum of 6-NB in *n*-hexane.

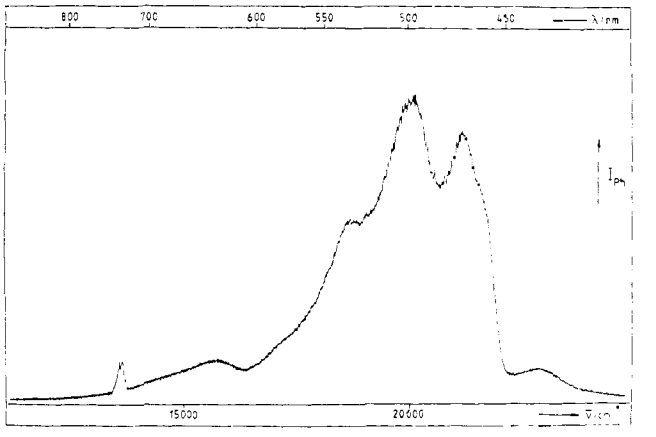

Figure 5. Phosphorescence spectrum of 6-NB in PMMA. (The weak band at 730 nm is due to the Hg-excitation line in second order.)

At $T \leq 4.2$ K, used throughout this work, the steps X ⇄ B are prohibited because of steric hindrance. Therefore, the first step can be taken as the starting point.

$$A \underset{\lambda_1(?)}{\overset{\lambda_1}{\rightleftharpoons}} X \qquad (2)$$

2. Experimental Section

The experimental investigation was conducted with an ODMR spectrometer which has been described elsewhere.[14] For excitation, the

(14) Bräuchle, Chr.; Kabza, H.; Voitländer, J.; Clar, E. *Chem. Phys.* **1978**, *32*, 63–73. Bräuchle, Chr.; Kabza, H.; Voitländer, J. *J. Phys. E.* **1980**, *13*, 302–305.

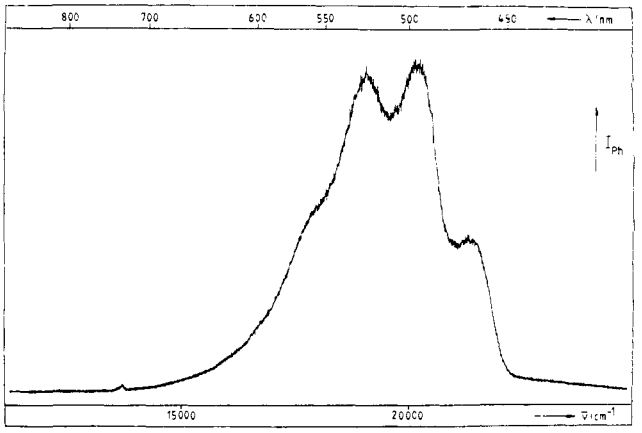

Figure 6. Phosphorescence spectrum of 6-NB in THF. (The weak band at 730 nm is due to the Hg-excitation line in second order.)

Table I. Analysis of the Emission Spectrum of 6-NB in 3-MP. Assignment of Spectral Regions to the Photochromic Forms and Vibrational Analysis of the A-Form Phosphorescence[a]

				assignment		
form	λ, nm	ν, cm^{-1}	Δν, cm^{-1}	1-subst benzene	NO_2 group	ref
A	458	21 834	(6737)			
	473	21 142	692		$2(a_1)$	680 cm^{-1} [38]
	480	20 833	1001	$1(a_1)$		1008 cm^{-1} [39]
	488 sh	20 492	1342		$1(a_1)$ or $2 \times 2(a_1)$	1320 cm^{-1} [26]
	493	20 284	1550		$4(b_2)$	1530 cm^{-1} [26]
	496 sh	20 161	1673	$1(a_1)$	$+2(a_1)$	
	503 sh	19 881	1953		$3 \times 2(a_1)$	
	510	19 608	2226		$4(b_2) + 2(a_1)$	
	518 sh	19 305	2529	$1(a_1)$	$+4(b_2)$	
	534	18 727	3107		$2 \times 4(b_2)$	
	538 sh	18 587	3247	$1(a_1)$	$+4(b_2)$	
	553 sh	18 083	3751		$2(a_1) + 2 \times 4(b_2)$	
	580	17 241	4593		$3 \times 4(b_2)$	

form	λ, nm	ν, cm^{-1}	Δν, cm^{-1}	assignment	ref
X	642	15 576	(7151)	phosphorescence	
B	689	14 514	(2015)	fluorescence	

[a] Δν values in parentheses give energetic distances to the long wavelength tails of the pertinent absorption spectra in Figure 2.

365-nm Hg line was used, i.e., λ_1 in Figure 2. Emission spectra were recorded at $T = 4.2$ K; for the ODMR experiments temperatures below 1.4 K were applied.

2.1. Sample Preparation. 6-NB was synthesized and purified according to the procedure given in ref 15. The following solvents were used to prepare solutions with concentrations of approximately 10^{-5} mol/L: (a) 3-methylpentane (Fluka pur., purified by twofold distillation over $LiAlH_4$), (b) *n*-hexane (Merck Uvasol for spectroscopy), (c) tetrahydrofuran (Merck Uvasol for spectroscopy), (d) methyl methacrylate (Fluka pur., purified by twofold distillation), with catalyst. The solutions were degassed by at least five freeze–pump—thaw cycles and sealed off under vacuum. The methyl methacrylate solution was polymerized by irradiating it for 2 days with a 60-W tungsten lamp. A similarly prepared sample of poly(methyl methacrylate) (PMMA) with catalyst but without 6-NB gave no emission.

2.2. Emission Spectra. The emission spectra of 6-NB in all solvents show only broad band vibrational structure, cf. Figures 3–6; therefore the vibrational analysis of the spectra given in Tables I–IV is accurate merely to about ±50 cm^{-1} for each band. The assignment of some vibrations to modes of benzene or toluene is based on our model for the electronic structure of 6-NB which will be described and justified in section 3.6. The benzene or toluene bands are given in Wilson's numbering;[16] the

(15) Berman, E.; Fox, R. E.; Thomson, F. D. *J. Am. Chem. Soc.* **1959**, *81*, 5605–5608.

Table II. Analysis of the Emission Spectrum of 6-NB in *n*-Hexane. Assignment of Spectral Regions to the Photochromic Forms and Vibrational Analysis of the A-Form Phosphorescence[a]

				assignment		
form	λ, nm	ν, cm^{-1}	Δν, cm^{-1}	1-subst benzene	NO_2 group	ref
A	458	21 834	(6737)			
	472	21 186	648		$2(a_1)$	680 cm^{-1} [38]
	493	20 284	1550		$4(b_2)$	1530 cm^{-1} [26]
	510	19 608	2226		$4(b_2) + 2(a_1)$	
	535	18 692	3142		$2 \times 4(b_2)$	

form	λ, nm	ν, cm^{-1}	Δν, cm^{-1}	assignment	ref
X	638	15 674	(7053)	phosphorescence	
B	690	14 493	(2026)	fluorescence	

[a] Δν values in parentheses give energetic distances to the long wavelength tails of the pertinent absorption spectra in Figure 2.

Table III. Vibrational Analysis of the Phosphorescence Spectrum of 6-NB (A Form) in PMMA

				assignment		
form	λ, nm	ν, cm^{-1}	Δν, cm^{-1}	1-subst benzene	NO_2 group	ref
A	461 sh	21 692				
	470	21 277	415	$11(b_1)$		475 cm^{-1} [39]
	489 sh	20 480	1242	$9(b_2)$		1165 cm^{-1} [39]
	497	20 121	1571	$8(b_2)$		1591 cm^{-1} [39]
	521	19 194	2498	$9(b_2) + 9(a_1)$		
	536	18 657	3035	$8(b_2) + 8(a_1)$		

Table IV. Vibrational Analysis of the Phosphorescence Spectrum of 6-NB in THF

				assignment		
form	λ, nm	ν, cm^{-1}	Δν, cm^{-1}	1-subst benzene	NO_2 group	ref
A	467	21 413				
	495	20 202	1211	$9(b_2)$		1165 cm^{-1} [39]
	526	19 011	2402	$9(b_2) + 9(a_1)$		1185 cm^{-1} [39]
	561 sh	17 825	3588	$9(b_2) + 2 \times 9(a_1)$		
	602	16 611	4802	$9(b_2) + 3 \times 9(a_1)$		

NO_2 vibrations are numbered according to ref 17.

The nature of the emission bands was identified as fluorescence or phosphorescence by lifetime measurements. The solutions of 6-NB in tetrahydrofuran (THF) and PMMA showed phosphorescence only, which under prolonged irradiation (a few hours) did not change in shape but decreased in overall intensity. In the emission spectra of the *n*-hexane and 3-methylpentane (3-MP) solutions, three regions have to be distinguished: (i) Phosphorescence from about 21 000 to 17 000 cm^{-1} whose intensity decreases after a few hours irradiation; (ii) a phosphorescence band at 15 500 cm^{-1} which grows as (i) decreases; (iii) a strong fluorescence band at 14 500 cm^{-1} which also grows under irradiation (cf. Figures 3 and 4, and Tables I and II, especially Figure 3). Quantitative details of the underlying photochemical kinetics will be discussed elsewhere.[7] The assignment of these spectral regions to the various photochromic forms is given in Figure 3. It is based, first, on a comparison with the absorption spectra in Figure 2 (cf. the Δν values in brackets in Tables I and II) which are the energy differences between the emission band and the long wavelength absorption band of the assigned photochromic form, and second, on eq 2 with the forward reaction A → X being mainly operative. According to the considerations in section 1 the formation of B at 4.2 K has to be ruled out; the increase in the B fluorescence therefore is only apparent and is actually due to X phosphorescence extending into that region. However, at room temperatue

(16) Herzberg, O. "Molecular Spectra and Molecular Structure"; Van Nostrand-Reinhold: New York, 1945; Vol. II, p 363.
(17) Nakamoto, K. "Infrared Spectra of Inorganic and Coordination Compounds"; Wiley-Interscience: New York, 1970; p 160.

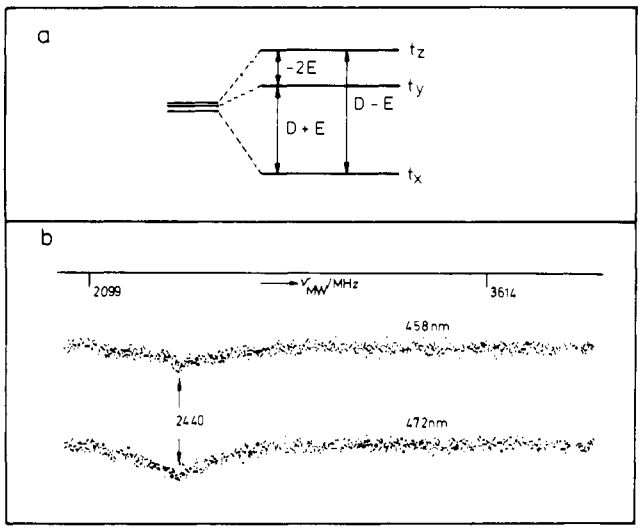

Figure 7. (a) Zero-field splitting and microwave transitions for $D > 0$, $E < 0$.[9] (b) $D + E$ transition of 6-NB (A form) in *n*-hexane (300 CAT cycles).

Table V. Microwave Transitions and Zero-Field Splitting Parameters of 6-NB in Various Solvents (Values in GHz)

solvent	form	transitions			$\|D\|$	$\|E\|$
n-hexane	A	4.3	2.4	1.8	3.4	0.9
	X	2.9	1.7	1.2	2.3	0.6
PMMA	A	4.7	3.2	1.6	3.9	0.8
	X	4.0	2.5	1.5	3.3	0.8
THF	A		2.8	1.8	3.7	0.9
	X	3.4	2.3	1.1	2.8	0.6

B *is* formed, when the samples are treated according to the following procedure.

The emission spectra of the *n*-hexane and the 3-MP solutions could be brought back to their preirradiation shape (solid line in Figure 2) by simply illuminating the samples at room temperature with a 60-W tungsten lamp for several hours (similarly the original emission intensity of the THF and PMMA solution was reestablished). This procedure, however, which is based on eq 1 with additional thermal steps, leads merely to an equilibrium between A and B. Hence, B is present in the sample (after this treatment) even at 4.2 K. Only the very first (virginal) emission spectra of the *n*-hexane and 3-MP samples did not show any fluorescence of form B.

2.3. ODMR Investigations. With the help of the well-known ODMR techniques[9,14] the (photophysical) properties of the lowest excited triplet state T_1 of 6-NB in its A and X form were investigated. Because no phosphorescence of B could be detected, ODMR measurements on the triplet state of this form were not possible.

Zero-Field Splitting. No microwave transitions could be detected in the 3-MP solutions of 6-NB. The transitions found with the other samples reflect the broad band features displayed by the emission spectra (zero-field splitting and typical signals are shown in Figure 7); some of the transitions of 6-NB in *n*-hexane could only be determined by an approximate procedure to an accuracy of about ±0.1 GHz. The zero-field splitting parameters D and E presented in Table V therefore are estimated to have error margins of ca. 0.1 GHz. It was not possible to obtain better signal-to-noise ratios by increasing the number of averaging cycles, because the phosphorescence intensity of 6-NB in *n*-hexane is poor already at the beginning of the irradiation and further decreases as the photoreaction A → X proceeds.

The assignment of D and E to the photochromic forms is unequivocal for the *n*-hexane sample only, because here A and X forms phosphoresce in different spectral regions (cf. Figure 4 and Table II). In THF and PMMA however, the X phosphorescence obviously is blue shifted and is hidden under the stronger A phosphorescence. Nevertheless, the two forms can be distinguished from their different zero-field splittings; in analogy to the *n*-hexane result the X form is assigned to the lower D value. This assignment will be justified by the discussion in section 3.7.

Photophysical Kinetics of T_1. The kinetic parameters of the triplet zero-field levels of 6-NB in its A and X form were determined for the *n*-hexane sample (cf. Table VI) with microwave-induced delayed phosphorescence (MIDP) techniques.[9] Up to 600 CAT cycles were necessary to obtain some of the signals; from their signal-to-noise ratio typical errors are estimated to be about 20%.

Table VI. Kinetic Parameters of T_1 of 6-NB (A and X form) in *n*-Hexane, Measured at 458, 473, and 642 nm[a]

	A (458 nm)			A (473 nm)			X (642 nm)		
	x	*y*	*z*	*x*	*y*	*z*	*x*	*y*	*z*
k, s^{-1}	2.4	8.1	20	2.3	8.1	20	3.7	17	(100)
k^r	7	100	14	4	100	14	2	100	(10)
N^0				53	100	(50)			
K				15	100	(130)			

[a] k, total deactivation rates; k^r, relative radiative deactivation rates; N^0, relative equilibrium (steady-state) populations; K, relative population rates.

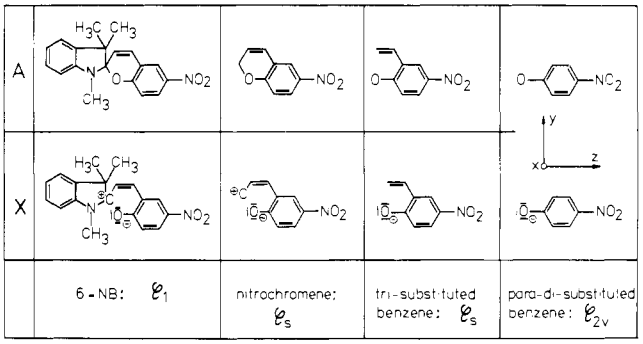

Figure 8. Models for the discussion of T_1 properties of 6-NB.

Values given in brackets are estimates. Generally, transitions involving the t_z level yielded only poor MIDP signals, due to two facts: (i) the radiative rates k^r_x and k^r_z are nearly identical within the error margin and (ii) for the *y*–*z* transition, a high enough conversion factor could not be achieved because of power limitations of our microwave equipment. Specifically, for the 473-nm band of the A phosphorescence the t_x–t_z transition could not be detected with CW ODMR spectroscopy. Here, the microwave frequency is swept slowly during the sample, which is irradiated continuously so that an equilibrium population of the T_1 sublevels is established. On the other hand, MIDP signals *could* be obtained. It follows that the (relative) steady-state populations N^0 of the t_x and t_z sublevels are very similar; hence the relative intersystem crossing rates K_z can also be estimated (cf. Table VI).

The t_x–t_z transition of the X form yielded very poor MIDP signals with a fast decay (~10 ms). From this the deactivation rate k_z was estimated. Under comparable conditions (especially microwave power and delay of the microwave pulse with respect to the turnoff of the excitation light) the t_x–t_y signal was higher than the t_x–t_z signal by a factor of more than 10. Hence, the relative radiative rate constant k^r_z is estimated to be about one tenth of k^r_y.

3. Discussion

The properties of the lowest excited states S_1 and T_1 of the photochromic spiropyrans have been investigated experimentally[18-20] and theoretically;[21-23] however, none of the cited papers deals with the intermediate X form. In this section, T_1 of *both* A and X forms will be discussed.

For the explanation of the experimental data, we propose the following model which will be developed in the next three subsections: The T_1 properties of A and X are governed by a very small part of 6-NB, namely, the para-disubstituted benzene unit.

3.1. From 6-NB to Trisubstituted Benzene. To begin with, from the orthogonality of the indoline (I) and nitrochromene (NC) parts of the molecule it is obvious to suppose that the excited-state wave functions of A or X can be written as products I·NC* or I*·NC.

(18) Becker, R. S.; Dolan, E. E.; Balke, D. E. *J. Chem. Phys.* **1969**, *50*, 239–245.
(19) Belaits, I. L.; Platonova, T. D. *Opt. Spektrosk.* **1973**, *35*, 218–223.
(20) Balny, C.; Mossé, M.; Audic, Ch.; Hinnen, A. *J. Chim. Phys.* **1971**, *68*, 1078–1083.
(21) Bărta, M. *Coll. Czech. Chem. Commun.* **1978**, *43*, 416–423.
(22) Tyutyulkov, N.; Stoyanov, S.; Taseva, M.; Schuster, P. *J. Signalaufzeichnungsmaterialien* **1975**, *3*, 435–442.
(23) Tinland, B. Gugliemetti, R.; Chalvet, O. *Tetrahedron* **1973**, *29*, 665–667.

Table VII. Admixture of C_6H_6 and CT Configurations (in %) Calculated for the Trisubstituted Benzene Model

	A form		X form	
	$S_0(A_1)$	$T_1(A_1)$	$S_0(A_1)$	$T_1(A_1)$
$^{1,3}\Psi^0{}_\varphi$	76.0	44.9	75.0	10.0
$\psi_1' \rightarrow 0$	6.4	39.7		
$O^- \rightarrow \psi_{-1}'$			2.4	0.2
$\psi_1' \rightarrow NO_2$	4.6	10.3	14.2	89.4
$C_6H_6 \leftrightarrow V^a$	4.7	2.1	5.1	0.3
other CT[b]	8.3	3.0	3.3	0.1

[a] In $C_6H_6 \leftrightarrow V$ all contributions are contained, where charge is transferred between the benzene ring and the vinyl group (V). [b] All other CT configurations which have been taken into account preserve C_{2v} symmetry but otherwise yield only minor contributions. They are therefore not shown explicitly.

This idea was confirmed by spectroscopic data[11] as well as by a CNDO–Cl calculation[23] for the A form, and both S_1 and T_1 were identified as I·NC*. We assume this to be true also for the X form.

The T_1 properties of A and X are determined by the nitrochrome part exclusively; the wave function, however, is not delocalized over the whole submolecule. First, evidence comes from the ODMR results giving strong hints by symmetry arguments that not the whole heteroring has to be taken into account. This will be discussed in detail in section 3.3. The following two observations further support this approach: (i) Simonetta and Pilar[24] calculated bond orders in furan and found nearly pure single bond character for the C–O bond. (ii) ODMR investigations on benzofuran could be discussed by Hirota et al.[25] by simply considering benzofuran as a disubstituted benzene: the T_1 wave function does not "see" the furan C–O bond.

In summary, we end up with a trisubstituted benzene (cf. Figure 8). Note, that in this model the only difference between A and X consists in the pyrane oxygen being charged or not.

3.2. Charge-Transfer Wave Functions. Starting with a trisubstituted benzene as a model system for the nitrochromene part, the question arises "Is the T_1 wave function delocalized into all three substituents, the pyran oxygen, the NO_2 group, and the vinyl group"? To give an answer, we carried out a calculation of charge-transfer (CT) admixtures to local benzene configurations (CT wave functions). The idea of CT configurations being essential for the description of the 6-NB triplet state was first discussed by Bârta[21] on the basis of a CNDO/2S calculation. However, he merely considered transfer into the NO_2 group, i.e., $a^3(\pi\pi_0^*)$ state. Here, π designates a benzene orbital whereas π_0 is a nonbonding orbital[26] located on one of the NO_2 oxygens which has π symmetry with respect to the nitrochromene plane.

In general, CT admixtures in substituted benzenes can be discussed in terms of the mesomeric effect.[27,28] As we did not take into account the inductive effect, excitation energies resulting from the calculations should not be taken too seriously; therefore they are omitted in Table VII. Details of the procedure have been given by Murrel,[27] so a brief review will suffice.

The zero-order configurations are pure benzene (φ) and CT states. the triplet wave function of benzene has been calculated by van der Waals[29]

$$3\Psi_\varphi = 0.966(\Psi_1^{-1} + \Psi_{1'}^{-1'})/\sqrt{2} + 0.255\Psi_2^{-2} \qquad (3)$$

where Murrell's notation[27] is adopted. The T_1 energy is taken from experiment:[30] $^3E_\varphi = 3.68$ eV. Among the possible CT configurations, direct transfer from a donor substituent to an acceptor substituent (D → A) is neglected; all reasonable ($\psi_i \rightarrow$ A) and (D → ψ_{-i}) configurations are allowed, where ψ_i and ψ_{-i} designate the appropriate bonding and antibonding benzene MOs, respectively. The CT energies can be calculated within the framework of the PPP procedure:

$$^3E_{CT} = I - A + C \qquad (4)$$

Ionization energies I and electron affinities A can be found in tables,[31] but the Coulombic part C has to be calculated. Here a simple point charge model is used, and it is at this stage that the specific molecule under consideration enters, namely, via its geometry. For the atomic coordinates in the chromene, we took the results from an extended Hückel calculation.[21] Note, that the spiro C atom is charged in the X form (cf. Figure 1); this has two consequences: (i) Its Coulomb interaction with the point charges generated by the CT makes important contributions to the CT energies, in general. (ii) Specifically, the strong interaction with the negatively charged pyran oxygen prevents CT from O^- to the benzene ring. Therefore, a quinoid structure can be excluded (cf. Figure 8). Another source of difference in CT energies between A and X form lies in the pyran oxygen itself: in the X form it is charged, and one has to use the ionization energy and the electron affinity of the O^- ion in eq 4.

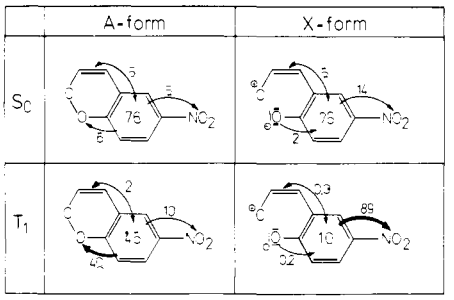

Figure 9. Results of the CT calculation (cf. Table VII). Numbers represent the admixture of C_6H_6 and CT configurations in % (rounded); the arrows indicate the direction of CT.

The zero-order configurations are mixed by matrix elements which can be evaluated very simply when overlap is neglected—cf. ref 27 for details. The configuration interaction matrices were diagonalized numerically. The results are presented in Table VII and, for clarity, pictured in Figure 9. The ground states were also included in the calculations in order to discuss solvent effects on 0–0 bands of phosphorescence (cf. section 3.5).

3.3. Symmetry and Electronic Nature of the Excited States. The results of the calculations show that the T_1 wave functions of both A and X get virtually no contributions from charge transfer between the benzene ring and the vinyl group (V). Therefore, they can be further factorized

$$T_1 = I{\cdot}V{\cdot}(pdB)^* \qquad (5)$$

and the T_1 properties are dominated by the para-disubstituted benzene (pdB) subunit of the 6-NB molecule. Now the symmetry group governing the dynamic properties of T_1 should be that of the pdB subunit: i.e., C_{2v}. The unique selection rules which can be derived within this group should then lead to very distinct population and deactivation characteristics for the triplet zero-field levels.[9,32] This prediction will be tested against experiment later. But, strictly speaking these symmetry considerations are approximations, and matrix elements for "forbidden" transitions do not vanish exactly; nevertheless, as long as the matrix elements get only minor contributions from those regions of space where

(24) Simonetta, M. *J. Chim. Phys.* **1952**, *49*, 68–76. Pilar, F. L. *J. Mol. Spectrosc.* **1960**, *5*, 72–77.
(25) Harrigan, E. T.; Hirota, N. *J. Am. Chem. Soc.* **1975**, *97*, 6647–6652.
(26) Feuer, H., Ed. "The Chemistry of the Nitro- and Nitroso-Groups" In "The Chemistry of Functional Groups"; Patai, S., Ed.; Wiley: New York, 1969; Vol. 5, Part 1, pp 39–48.
(27) Murrell, J. N. "The Theory of The Electronic Spectra of Organic Molecules"; Methuen: London, 1963.
(28) Kimura, K.; Tsubomura, H. *Mol. Phys.* **1966**, *11*, 349–358.
(29) Van der Waals, J. H.; ter Maten, G. *Mol. Phys.* **1964**, *8*, 301–317.
(30) Bernstein, E. R.; Colson, S. D.; Tinti, D. S.; Robinson, G. W. *J. Chem. Phys.* **1968**, *48*, 4632–4659.
(31) Weast, R. C., Ed. "CRC Handbook of Chemistry and Physics, 59th ed.; Chemical Rubber Publishing Co.: Cleveland, OH, 1978/79.
(32) Bräuchle, Chr.; Kabza, H.; Voitländer, J. *Chem. Phys.* **1981**, *55*, 137–152.

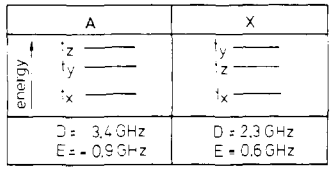

Figure 10. Energetic sequence of zero-field levels and sign of ZFS parameters of 6-NB in *n*-hexane.

symmetry is broken, selection "rules" can be used even in an approximate symmetry group.

From ODMR experiments the symmetry properties of the T_1 wave function can be evaluated.[9,14,32] If the whole nitrochrome has to be taken into account, or—in the former model of trisubstituted benzene—if the vinyl group is also allowed to make contributions, the appropriate point group would be C_s. Within C_s, however, the population and deactivation characteristics of the two inplane triplet sublevels are similar. This is not borne out by the data of Table VI. For the 0–0 band, only one zero-field level is responsible for radiative deactivation of the triplet state of the A form, and the same has to be supposed for the X form, as is discussed in section 2.3. In connection with the vibrational structure of the phosphorescence spectra (cf. section 3.5.), this behavior can only be explained by attributing a higher point group to the triplet wave function.

From an unprejudiced inspection of the nitrochromene, one would expect C_{2v}, D_{2h}, and D_{6h} to be suitable as well. The two D groups, however, can be ruled out immediately: They would be connected with virtually pure benzenoid configurations (perhaps slightly distorted), which in turn result in characteristic spectroscopic features,[33] e.g., a very weak 0–0 band and a vanishing E parameter. These are not displayed by the data shown in Figures 3–6 and Table V. Hence, in excellent agreement with the calculations, the experimental results also require C_{2v} as the appropriate symmetry group for the description of T_1 (A and X).

Within this group, there are distinct selection rules which can be used in the spirit of the above-mentioned proviso. In particular, they require the triplet space symmetry to be of A_1 or B_2 nature, i.e., $\pi\pi^*$, if only one zero-field level is radiating into the 0–0 band.[9] Therefore, T_1 of both A and X is identified unequivocally as a $\pi\pi^*$ state—in agreement with recent assignments given, however, only for the A form.[18,21]

From the ODMR experiments alone, A_1 and B_2 space symmetries cannot be distinguished. At this point, and justified by the success of the underlying model which will become apparent in the following, we use the result of the calculation: the orbital part of T_1 of both the A and the X form transforms like A_1. A simple group theoretical consideration[9] then yields the energetic sequence of the zero-field levels and the (relative) sign of the zero-field splitting parameters (cf. Figure 10).

To summarize, the results of CT calculations as well as ODMR investigations of 6-NB in *n*-hexane show that the lowest excited triplet states of both A and X form can be described consistently by taking into account the para-disubstituted benzene submolecule solely (cf. Figure 8).

3.4. Solvent Effects. In inert solvents like *n*-hexane, the T_1 and S_0 wave functions of 6-NB have CT admixtures as shown in Table VII and Figure 9. In THF and PMMA, on the other hand, the transfer of an electron to the NO_2 group is blocked. This is readily understood when one considers an MO diagram or the resonance structures of nitrobenzene,[26] from which it can be inferred that the nitrogen possesses a merely half-filled p orbital. The solvent properties of THF and PMMA, on the other hand, are characterized to a large extent by nonbonding electrons located at the oxygen of the solvent molecule, which can form a strong donor–acceptor bond with the electron-accepting part of the solute—i.e., in the case of 6-NB the nitrogen of the NO_2 group. Now the nitro group is negatively charged: hence the transfer of additional negative charge from the benzene ring is virtually inhibited.

Clearly, other electron-accepting parts of the 6-NB molecule could also be involved in solute–solvent interactions but—as will become apparent in the following subsection—the interaction with the NO_2 group makes the major contribution to the solvent effects. In particular, it is to be supposed that the attack of the solvent donor is not favored in the vicinity of the spiro C atom because of steric hindrance.

The most important effect of using THF or PMMA as solvents therefore is the blocking of the charge transfer from the benzene ring to the NO_2 group. There are two consequences: (i) the wave functions are more localized and (ii) the state energies are altered.

3.5. 0–0 bands of Phosphorescence. The energetic aspect is considered first, and it is at this point only that use is made of the S_0 wave functions in Table VII and Figure 9. State energies in general will be increased when CT to one of the substituents is blocked: full stabilization via configuration interaction is no longer possible, or in the more intuitive terms of valence bond theory, one stabilizing resonance structure is missing.

Therefore, the wavelength of the 0–0 band of phosphorescence will show any solvent effect, in general, a blue or a red shift, or none, depending on whether S_0 or T_1 is destabilized, or otherwise to what degree the admixture of $C_6H_6 \rightarrow NO_2$ to the pertinent wavefunctions occurs (cf. Table VII and Figure 9).

In the A form, S_0 and T_1 are contaminated with this configuration to nearly the same—rather low—degree. When using a CT blocking solvent instead of an inert one, both states suffer an only small and nearly equal destablization: the phosphorescence 0–0 bands of 6-NB (A form) are expected to be virtually of the same wavelength in *n*-hexane and 3-MP on the one hand and in PMMA and THF on the other. This is actually borne out by the experiment, cf. Tables I–IV, $\Delta\nu \sim 500$ cm^{-1}.

For the X form, there is indirect but nevertheless convincing experimental evidence for a substantial blue shift of the 0–0 band. For the *n*-hexane and 3-MP samples, the band could be identified from the phosphorescence spectra unequivocally, cf. Figures 3 and 4 and Tables I and II. For the PMMA and THF samples, the X phosphorescence is hidden under the stronger A phosphorescence (as indicated by the ODMR results, cf. section 2.3.); the blue shift therefore is of the order of 5000 cm^{-1}. This fact is in full accord with the degree of $C_6H_6 \rightarrow NO_2$ admixtures to S_0 and T_1 of the X form shown in Table VII, predicting that T_1 will be destabilized considerably more than S_0 in the CT blocking solvents.

3.6. Vibrational Structure of Phosphorescence. A further consequence of the inhibition of the charge transfer to the NO_2 group is the diminished spatial extent of the wave function. In the following subsection this will be discussed quantitatively for T_1. Here it is shown that this concept can also be used to analyze consistently the phosphorescence vibrational structure of 6-NB in various solvents.

The vibrational analyses given in Tables I–IV are based on frequency values taken from the literature (cf. the table entries on the right). It was not possible to support the assignments, determining the symmetry of the bands, by ODMR experiments[9,32] because of the broad band features of the phosphorescence.

The analyses were guided by the proposed model of a substituted benzene subunit for 6-NB. Accordingly, the phosphorescence bands were grouped into substituent and benzene-like vibrations. It turned out however, vide infra, that among the substituents only NO_2 can be seen in the spectra. Therefore, a monosubstituted benzene model suffices as far as the vibrational structure is concerned, and toluene data could by used for the assignment of the benzene-like bands.

The 1000-cm^{-1} band seen in the spectrum of the 3-MP sample is the basis of progressions with vibrations which are to be assigned to the NO_2 group unequivocally (cf. Table I). It therefore cannot be considered as the C_{spiro}–O vibrations (954 cm^{-1} [34]) because no benzene vibration manifests itself which could help in mechanically coupling the motions in the two distant substituents. This con-

(33) Bräuchle, Chr.; Deeg, F. W.; Voitländer, J. *Chem.* Phys. **1980**, *53*, 373–381. Deeg, F. W.; Bräuchle, Chr.; Voitländer, J. *Ibid.* **1982**, *64*, 427–436.

(34) Schiele, C.; Arnold, G. *Tetrahedron Lett.* **1967**, *47*, 1191–1195.

Table VIII. Zero-Field Splitting Parameters of 6-NB (in GHz), Calculated from CT Wave Functions (cf. Table VII), As Compared to the Experimental Values for the *n*-Hexane Solution

	A form	X form
% CT	55.1	90.0
D_{calcd}	3.40	2.52
D_{exptl}	3.4	2.3
E_{calcd}	−1.52	−2.48
E_{exptl}	−0.9	+0.6

clusion is also in accord with C_{2v} symmetry: the spiro band could not be attributed to one of the C_{2v} irreducible representations. Hence the band was assigned to a totally symmetric vibration of the 1-substituted benzene unit.

The 1550-cm^{-1} band which is found in all spectra cannot be the C=C stretching vibration of the vinyl group[25] because of reasons analogous to the above mentioned. For inert solvents, the band was assigned to the asymmetric valence vibration of NO_2.[17] For the CT blocking solvents PMMA and THF, the matrix elements of radiative deactivation get no contributions from the region of the NO_2 group; therefore the band was assigned to a benzene vibration.

Another interpretation which cannot be ruled out, but would not contradict our model, is that for all solvents this band is due to the typical ν_8 benzene vibration.[16]

3.7. Zero-Field Splitting of T_1. The value of the D parameter is determined by the spatial extent of the T_1 wave function:[35] when the delocalization region diminishes, D increases. Hence it is to be expected that for the CT blocking solvents (PMMA and THF) the D values of 6-NB both in its A and in its X form are higher than for the *n*-hexane sample. This is actually borne out by the data in Table V.

Additional justification that CT configurations are essential for understanding the T_1 properties of 6-NB comes from ESR measurements carried out in ethanol solutions.[36] In this solvent CT is not blocked, but enhanced: the electron is drawn via the NO_2 group to the hydroxyl of the ethanol because of a strong solvent–solute hydrogen bond. Therefore D should be lower than in an inert solvent; actually it was measured to be 2.80 GHz.[36] According to the experimental conditions quoted in ref 36, this value has to be assigned to the A form.

The relation between the degree of CT character admixed into the T_1 wave function and the value of the D parameter has been evaluated quantitatively by Godfrey, Kern, and Karplus.[37] In particular, they calculated D for a 100% CT configuration of a monosubstituted benzene (with point-like substituent) to be D_{CT} = 2.27 GHz. For mixed configurations, a linear relation is assumed:

$$D = D_\varphi + (D_{CT} - D_\varphi) \times \%CT/100 \qquad (6)$$

D_φ is the value for benzene, which was taken from experiment: D_φ = 4.78 GHz.[37] Analogous arguments are valid for the E parameter with E_φ = 0 and E_{CT} = 2.75 GHz. Therefore, from the CT wave functions of Table VII, D and E for both the A and X forms could be calculated (cf. Table VIII). The value for D agrees well with those measured for the *n*-hexane sample, but the E parameters—which are difficult to calculate in general—come out too negative. Here the limitations of the model become apparent. The NO_2 group is far from being point-like as was assumed in subsection 3.2. but extends considerably into the $\pm y$ direction (cf. Figure 8 for the axis system chosen). The E parameter is mainly determined by the expectation value of y^2-z^2, y and z being components of the vector connecting the two triplet electrons.[9,32] Hence, it is clear that the measured E's will be more positive compared to the calculated ones, the higher the degree of $C_6H_6 \rightarrow NO_2$ admixture to the triplet wavefunctions. Therefore, it is not surprising that E of the X form actually was found to be positive.

Note that the good agreement between the calculated and the measured D values strongly supports the model of a para-disubstituted benzene. If the T_1 wave functions of 6-NB were supposed to extend over the whole nitrochromene, one could not explain the decrease in D when the pyran ring is opening. Instead, using $D \propto r^{-3}$ which is approximately valid for planar molecules (r being the distance of the triplet electrons), one would predict the D value of the X form to be higher than for the A form.

4. Conclusion

6-Nitrobenzospiropyran was investigated by means of emission spectroscopy and ODMR; the experimental data obtained were discussed within a model based on a calculation of CT wave functions. The results can be rationalized as follows:

(1) The photochromic reaction does not take place at the very low temperatures used throughout this work—the colored planar B form is not obtained from the uncolored spiro A form because of steric hindrance. Instead, the reaction sequence is interrupted after the primary photochemical step, the formation of the long-suspect intermediate X form, where the orthogonal spiro topology still is retained. Both the A and the X form phosphoresce and could be identified from the emission spectra and the zero-field splitting measurements.

(2) The properties of A and X are determined by a small portion of the 6-NB molecule, viz., the para-disubstituted benzene subunit of the chromene part. First, evidence comes from the kinetic ODMR investigations which yielded deactivation rates typical for C_{2v} symmetry as opposed to the trivial C_1 or C_s which would have been expected. Secondly, a calculation of charge-transfer wave functions was carried out. It is based on the fact that the central benzene unit of the nitrochromene part does not "see" the whole oxygen-containing heteroring anneallated to it; instead the nitrochromene can be viewed as a trisubstituted benzene. The results show that one of the substituents, the vinyl group, plays a negligible role—i.e., only a para-disubstituted benzene unit, which obviously has C_{2v} symmetry, is responsible for the T_1 properties.

(3) The para-disubstituted benzene model—surprising as it seems—together with the quantitative results of the CT calculations can explain nearly all experimental data. The solvent effects on the 0–0 bands and the vibrational structure of the phosphorescence as well as the zero-field splitting parameters for both the A and the X form are all due to a blocking (or an enhancement) of the charge transfer $C_6H_6 \rightarrow NO_2$. On the other hand, the differences between the properties of A and X, for all solvents used, can be traced back to the different wave functions. Finally, from the degree of CT admixture to the T_1 wave functions, the zero-field splitting parameters D and E were calculated and compared with the experimental data gained from an inert solvent sample. For the D parameter, which measures the spatial extent of the T_1 wave function, the agreement is striking, and the relation $D(A) > D(X)$, which would not have been expected at first sight, comes out correct. The bad agreement between the measured and calculated E values indicates the limitations of the model; however, even these deviations can be explained in tendency and in extent with the model of the para-disubstituted benzene and the results of the CT calculations.

(4) The following statement therefore seems to be justified: The photophysical properties of the lowest excited triplet state T_1 of 6-NB (A and X) are governed by locally excited benzene configurations and considerable degrees of CT admixture as well as by the selection rules of the C_{2v} point group. Even though the

(35) Bräuchle, Chr.; Kabza, H.; Voitländer, J. *Chem. Phys.* **1980**, *48*, 369–385.

(36) Balny, C.; Santus, R.; Douzou, P. *C.R. Hebd. Seances Acad. Sci. Ser. C* **1966**, *262*, 1311–1314.

(37) Godfrey, M.; Kern, C. W.; Karplus, M. *J. Chem. Phys.* **1966**, *44*, 4459–4469. Use of recent results (Matsui, K.; Morita, H.; Nishi, N.; Kinoshita, M.; Nagakura, S. *J. Chem. Phys.* **1980**, *73*, 5514–5520) which differ from those obtained by Godfrey, Kern and Karplus would not affect our argument in its essence.

(38) Landolt-Börnstein "Zahlenwerte und Funktionen aus Physik, Chemie, Astronomie, Geophysik und Technik"; Springer: Berlin, 1951; Vol I, Part 2.

(39) Haaland, D. M.; Nieman, G. C. *J. Chem. Phys.* **1973**, *59*, 4435–4457.

phosphorescent and the reactive triplet states need not necessarily be identical, the above features can serve as a first guideline for the investigation of the photochemical properties of 6-NB, which is currently under way.

Acknowledgment. We thank Professor Dr. H. Rau from the University of Stuttgart-Hohenheim for valuable discussions. A grant to M.G. from the Deutsche Forschungsgemeinschaft is gratefully acknowledged.

Ligand, Oxygen, and Carbon Monoxide Affinities of Iron(II) Modified "Capped" Porphyrins

Toshiaki Hashimoto,[1a] Robert L. Dyer,[1b] Maxwell J. Crossley,[1b] Jack E. Baldwin,[1b] and Fred Basolo*[1a]

Contribution from the Departments of Chemistry, Northwestern University, Evanston, Illinois 60201, and The University, Oxford OX1 3QY, England. *Received July 27, 1981*

Abstract: Ligand, O_2, and CO binding constants are presented for iron(II) modified "capped" porphyrins. Steric effects at the axial position outside the cap were altered by changing a tetraphenyl-type cap to a corresponding tetranaphthalene-type cap. The steric hindrance caused by the peri hydrogens of the naphthalene groups is believed to be responsible for the decrease in ligation in the order *n*-propylamine > isobutylamine > *sec*-butylamine > *tert*-butylamine. Inductive effects in the porphyrin plane were altered by introducing a nitro group. Such an electron-withdrawing group enhances ligation but retards oxygenation. The solvent effect on O_2 binding by the capped complexes is small, presumably because the environment of the O_2 bound inside the cap is not greatly changed by changes in solvent. The CO affinities of iron(II) capped porphyrins and of corresponding iron(II) flat-open porphyrins are similar. In contrast, the O_2 affinities of the capped systems are lower than their flat-open counterparts, which means the iron(II) capped porphyrin complexes discriminate against O_2 but not CO. This is discussed in terms of distal steric effects on the stable structures of Fe–O–O (bent) and Fe–C–O (linear).

Coordination chemists had been frustrated for many years due to their inability to prepare an iron complex capable of carrying oxygen in a manner akin to the natural proteins myoglobin and hemoglobin.[2] This frustration ended a few years ago with the discoveries that synthetic iron(II) complexes of "chelated-heme",[3] "picket-fence",[4] and "capped"[5] porphyrins reversibly add dioxygen. Since there are severe restrictions on studies that can be made on natural proteins, it is extremely important now to have these model oxygen carriers which can be subjected to the desired investigations. Extensive work has been done on the bonding and the structure of Fe–O_2 and of Fe–CO in these models[2,6] and on the kinetics and thermodynamics of ligation,[7-11] oxygenation,[6,8,11-14] and carbonylation.[11,14-16]

Our previous publications presented thermodynamic data on ligand[9] and on oxygen[13] affinities of iron(II) "capped" porphyrins. The data showed that ligand affinities are smaller relative to the corresponding "flat-open" porphyrin Fe(TPP),[17] and oxygen affinity is smaller than that of the picket-fence complex and the hemoproteins. This was rationalized in terms of conformational strain present in the capped systems. The data also reported the effect of axial ligation on oxygen affinity as well as the effect of cap size (n = 2 vs. 3 in Figure 1) on ligation and on oxygenation.

This paper reports the effect of electronic and of steric changes in the equatorial plane of the porphyrin ring on the addition of axial ligands, of oxygen, and of carbon monoxide in iron(II) modified capped porphyrins. The data reported show that the oxygen affinities of the capped porphyrin systems are less than those of the corresponding flat-open porphyrins, whereas the carbon monoxide affinities of both systems are similar. This

(1) (a) Northwestern University. (b) Oxford University.
(2) Jones, R. D.; Summerville, D. A.; Basolo, F. *Chem. Rev.* **1979**, *79*, 139–179.
(3) Chang, C. K.; Traylor, T. G. *J. Am. Chem. Soc.* **1973**, *95*, 5810–5811.
(4) Collman, J. P.; Gagne, R. R.; Halbert, T. R.; Marchon, J. C.; Reed, C. A. *J. Am. Chem. Soc.* **1973**, *95*, 7868–7870.
(5) Almog, J.; Baldwin, J. E.; Huff, J. *J. Am. Chem. Soc.* **1975**, *97*, 227–228.
(6) Collman, J. P. *Acc. Chem. Res.* **1977**, *10*, 265–272 and references therein.
(7) (a) Brault, D.; Rougee, M. *Biochem. Biophys. Res. Commun.* **1974**, *57*, 654–659. (b) Brault, D.; Rougee, M. *Biochemistry* **1974**, *13*, 4591–4597.
(8) Collman, J. P.; Brauman, J. I.; Doxsee, K. M.; Hablert, T. R.; Suslick, K. S. *Proc. Natl. Acad. Sci. U.S.A.* **1978**, *75*, 564–568.
(9) Ellis, P. E., Jr.; Linard, J. E.; Szymanski, T.; Jones, R. D.; Budge, J. R.; Basolo, F. *J. Am. Chem. Soc.* **1980**, *102*, 1889–1896.
(10) (a) Traylor, T. G.; Stynes, D. V. *J. Am. Chem. Soc.* **1980**, *102*, 5938–5939. (b) Traylor, T. G.; Campbell, D.; Tsuchiya, S.; Mitchell, M.; Stynes, D. V. *Ibid.* **1980**, *102*, 5939–5941. Note that our useage of peripheral steric effect differs from that of Traylor,[10b] who defines it as "steric effect encountered by more distant (72) groups in the (axially bound) ligand".
(11) Collman, J. P.; Brauman, J. I.; Collins, T. J.; Iverson, B.; Sessler, J. L. *J. Am. Chem. Soc.* **1981**, *103*, 2450–2452.
(12) (a) Traylor, T. G.; Chang, C. K.; Geibel, J.; Berzinis, A.; Mincey, T.; Cannon, J. *J. Am. Chem. Soc.* **1979**, *101*, 6716–6731. (b) Traylor, T. G.; Berzinis, A. P. *Proc. Natl. Acad. Sci. U.S.A.* **1980**, *77*, 3171–3175.
(13) Linard, J. E.; Ellis, P. E., Jr.; Budge, J. R.; Jones, R. D.; Basolo, F. *J. Am. Chem. Soc.* **1980**, *102*, 1896–1904.
(14) Traylor, T. G.; Mitchell, M. J.; Tsuchiya, S.; Campbell, D. H.; Stynes, D. V.; Koga, N. *J. Am. Chem. Soc.* **1981**, *103*, 5234–5236 and references therein.
(15) Rougee, M.; Brault, D. *Biochemistry* **1975**, *14*, 4100–4106 and references therein.
(16) Ward, ,B.; Wang, C. B.; Chang, C. K. *J. Am. Chem. Soc.* **1981**, *103*, 5236–5238.
(17) Abbreviations: Por, dianion of porphyrin; C_2-Cap, dianion of the C_2-capped porphyrin 5,10,15,20-[pyromellitoyltetrakis[*o*-(oxyethoxy)-phenyl]]porphyrin; C_3-Cap, dianion of the C_3-capped porphyrin 5,10,15,20-[pyromellitoyltetrakis[*o*-(oxypropoxy)phenyl]]porphyrin; NapC_2-Cap, dianion of the naphthyl C_2-capped porphyrin (see Figure 1); C_2-Cap-NO_2, dianion of the β-nitro C_2-capped porphyrin (see Figure 1); TPP, dianion of *meso*-tetraphenylporphine; T(*p*-OCH_3)PP, dianion of *meso*-tetrakis(*p*-methoxyphenyl)porphine; TpivPP, dianion of the "picket-fence" porphyrin *meso*-$\alpha,\alpha,\alpha,\alpha$-tetrakis[*o*-(pivalamido)phenyl]porphyrin; Piv$_3$(5ClmP)Por, dianion of the "tailed picket-fence" porphyrin *meso*-(α,α,α-tris[*o*-(pivalamido)phenyl]-β-[*o*-[5-(*N*-imidazolyl)valeramido]phenyl]-porphyrin; PocPivP, dianion of "picket-pocket" porphyrin (see ref 11 and structure in following paper); chelated protoheme (mesoheme), see ref 3; 6,6-cyclophane and 7,7-cyclophane, see ref 10 and structure in following paper; Mb, myoglobin; Hb, hemoglobin; B, monodentate ligand; 1-MeIm, 1-methylimidazole; 1,2-Me_2Im, 1,2-dimethylimidazole; 2-MeIm, 2-methylimidazole; 1,5-DCIm, 1,5-dicyclohexylimidazole; *n*-$PrNH_2$, *n*-propylamine; *i*-$BuNH_2$; isobutylamine; *sec*-$BuNH_2$, *sec*-butylamine; *t*-$BuNH_2$; *tert*-butylamine; THF, tetrahydrofuran; DMF, *N,N*- dimethylformamide; K^B, the equilibrium constant for the base addition Fe(Por) + B $\rightleftharpoons$ Fe(Por)B; $K_B{}^B$, the equilibrium constant for the base addition Fe(Por)B + B $\rightleftharpoons$ Fe(Por)B_2; $P_{1/2}{}^{O_2}$, the O_2 pressure at half-saturation; $P_{1/2}{}^{NH_3}$, the NH_3 pressure at half-saturation; CTAB, cetyltrimethylammonium bromide.

0002-7863/82/1504-2101$01.25/0